International Journal of Biochemistry and Cell Biology 112 (2019) 123–133

Contents lists available at ScienceDirect

International Journal of Biochemistry and Cell Biology

journal homepage: www.elsevier.com/locate/biocel

Studying the ShcD and ERK interaction under acute oxidative stress conditions in melanoma cells

Samrein B.M. Ahmed[a,b,c,*], Sara Amer[b], Mira Emad[b], Mohamed Rahmani[a,b], Sally A. Prigent[c]

[a] Sharjah Institute for Medical Research, University of Sharjah, United Arab Emirates
[b] College of Medicine, University of Sharjah, United Arab Emirates
[c] Molecular and Cell Biology Department, University of Leicester, UK

ARTICLE INFO

Keywords:
ShcD
ERK
Hydrogen peroxide
Oxidative stress

ABSTRACT

The newly identified melanoma-associated adaptor ShcD was found to translocate to the nucleus upon hydrogen peroxide treatment. Therefore, the aim of this study was to identify the ShcD network in melanoma cells under oxidative stress. LC–MS/MS and GFP-trap were performed to study the ShcD phosphorylation status during acute severe oxidative stress. ShcD was found to be phosphorylated at threonine-159 (Thr159) in response to 5 mM H_2O_2 treatment. The GPS 2.1 phosphorylation prediction program predicted that the Thr159Pro motif, housed in the N-terminus of the ShcD-CH2 domain, is a potential phosphorylation site for MAPKs (ERK, JNK or p38). Co-immunoprecipitation experiments revealed that ShcD mainly interacts with ERK in B16 and MM138 melanoma cells under both hydrogen peroxide-untreated and -treated conditions. Moreover, ShcD interacts with both phosphorylated and un-phosphorylated ERK, although the interaction between ShcD and phospho-ERK was primarily observed after H_2O_2 treatment. A MEK inhibitor (U0126) enhanced the interaction between ShcD and unphosphorylated ERK under oxidative stress conditions. Furthermore, Thr159 was mutated to either alanine (A) or glutamic acid (E) to study whether the threonine phosphorylation state influences the ShcD/ERK interaction. Introducing the T159E mutation obliterated the ShcD/ERK interaction. To identify the functional impact of the ShcD/ERK interaction on cell survival signalling under oxidative stress conditions, caspase 3/7 assays and 7AAD cell death assays were used. The ShcD/ERK interaction promoted anti-survival signalling upon exposure to hydrogen peroxide, while U0126 treatment reduced death signalling. Our data also showed that the death signalling initiated by the ShcD/ERK interaction was accompanied by p21 phosphorylation. In summary, these data identified ShcD, via its interaction with ERK, as a proapoptotic protein under oxidative stress conditions.

1. Introduction

Although reactive oxygen species (ROS) serve physiological roles in the immune response and act as signalling molecules in response to cellular stress, ROS accumulation contributes to many disease conditions, including neurodegenerative diseases, ageing, myocardial reperfusion injury, and cancer (Belikov et al., 2015; Martindale and Holbrook, 2002; Emerit et al., 2004; Kregel and Zhang, 2007; Hori and Nishida, 2009; Esme et al., 2008). Depending on its levels, ROS can activate specific signalling pathways that either protect the cells against death or trigger cell death signalling (Zhou et al., 2005; Trachootham et al., 2008). In contrary to the ROS function in activating different signalling pathways to promote carcinogenesis, ROS-induced cell death was observed in chemotherapy-treated cancer cells. ROS generation was also proposed as a mechanism to kill drug-resistant cancer cells (Wang et al., 2018).

Mitogen-activated protein kinases (MAPKs), including ERK, p38 and JNK, are key regulators of cellular responses to oxidative stress (Matos et al., 2005; Ruffels et al., 2004; Wang et al., 2003, 2011; Zhuang et al., 2007). The roles of the MAPKs in the oxidative stress response are partially achieved via phosphorylation of p66ShcA (Khalid et al., 2016; Hu et al., 2005), a member of the Src homology and collagen (Shc) family of adaptor proteins; the Shc family consists of four proteins with different functions: ShcA, B, C, and D (Fagiani et al., 2007). The diversity of the Shc protein functions depends on their different domains. Shc proteins contain two domains that allow them to dock with

Abbreviations: Shc, Src homology and collagen; ERK, extracellular signal–regulated kinase; JNK, c-Jun N-terminal kinase; ROS, reactive oxygen species; MAPK, mitogen activated protein kinase; GFP, green fluorescence protein; GAPDH, glyceraldehyde 3-phosphate dehydrogenase; HEK 293, human embryonic kidney cell line 293; Thr, threonine; Ser, serine; Pro, proline

* Corresponding author at: Sharjah Institute for Medical Research, University of Sharjah, United Arab Emirates.
E-mail address: samahmed@sharjah.ac.ae (S.B.M. Ahmed).

https://doi.org/10.1016/j.biocel.2019.05.009
Received 7 January 2019; Received in revised form 10 May 2019; Accepted 13 May 2019
Available online 20 May 2019

tyrosine-phosphorylated motifs, specifically a phosphotyrosine binding domain (PTB) and a Src homology 2 domain (SH2). These two domains are bridged by a collagen homology 1 domain (CH1), which mainly binds to Grb2 and facilitates the recruitment of proline-rich proteins (Ravichandran, 2001). Collagen homology 2 domain (CH2) is present only in the long isoforms of the Shc family members (Ravichandran, 2001). The CH2 domain is the least-studied element of the Shc proteins, although it has potential significance for ShcA function. p66ShcA, the longest isoform of ShcA, is phosphorylated at Ser36 under oxidative stress conditions downstream of p53 (Migliaccio et al., 1999). p66ShcA then participates in cytochrome C release from the mitochondria and inhibits forkhead proteins to induce apoptosis (Migliaccio et al., 1999; Giorgio et al., 2005; Nemoto and Finkel, 2002).

The most recently identified member of the Shc adaptor protein family, ShcD, is upregulated in invasive melanoma, enhances melanoma cell migration via MAPK-dependent and MAPK-independent pathways, and promotes melanoma tumorigenesis (Fagiani et al., 2007). Like p66ShcA, ShcD contains a CH2 domain with serine and threonine residues that are potential phosphorylation sites for various kinases. Moreover, ShcD was found to translocate to the nucleus following 5 mM H_2O_2 treatment (Ahmed and Prigent, 2014). Therefore, we sought to investigate the ShcD phosphorylation status following H_2O_2 treatment to reveal the molecular mechanism underlying the oxidative stress responses associated with the ERK, p38 and JNK mitogen-activated protein kinases in melanoma cells.

2. Methodology

2.1. Constructs, antibodies, and chemicals

FLAG and GFP-tagged ShcD were generated by Protex, University of Leicester, as previously described by Ahmed and Prigent (2014). pCMV3-*N*-FLAG Negative Control Vector and ERK2 cDNA ORF Clone, Human, C-GFPSpark® tag were obtained from Sinobiological (China). The following primary antibodies were used for western blotting: anti-FLAG (F1804; Sigma Aldrich, UK), anti-p44/42 MAPK(Erk1/2) (9102; Cell Signaling, USA), anti-phospho-p44/42 MAPK (Erk1/2) (4370S; Cell Signaling, USA), anti-p38 MAPK (8690; Cell Signaling, USA), anti-phospho-p38 MAP Kinase (9211; Cell Signaling, USA), anti-SAPK/JNK (9252; Cell Signaling, USA), anti-phospho-SAPK/JNK (9255; Cell Signaling, USA), anti-β actin (4970S; Cell Signaling, USA), anti-GAPDH (ab37168; Abcam, UK), anti-phopsho-p21(Thr145) (sc-20220; santa cruz; USA), and anti-phospho-threonine-proline (9391; Cell Signaling, USA). Horseradish peroxidase-conjugated anti-mouse (7076S; Cell Signaling, USA) and anti-rabbit (7074S; Cell Signaling, USA) secondary antibodies were used for immunoblotting. The T159E and T159A mutations were generated using the QuikChange II Site-directed mutagenesis kit (Agilent; US).

2.2. Cell maintenance and transfection

The HEK 293 cells stably expressing GFP-ShcD were generated by Samrein BM Ahmed at the University of Leicester, UK. The parental HEK 293 cells were a gift from Terry Herbert, University of Leicester, UK. The B16 cell line was a gift from Dr. Salem Chouaib of the Institut de Cancérologie Gustave Roussy-Villejuif, France. The MM138 human melanoma cell line was purchased from Sigma Aldrich, UK (ECACC collection). All of the reagents for cell growth and maintenance were obtained from Sigma Aldrich, UK. The B16 mouse melanoma cells and the HEK 293 cells were cultured in Dulbecco's Modified Eagle's Medium (D6429) supplemented with 10% foetal bovine serum (F9665) and 1% penicillin-streptomycin antibiotic solution (P4333). The MM138 human melanoma cells were cultured in RPMI 1640 medium (R8758) supplemented with 25 mM HEPES, 10% FBS and 1% penicillin-streptomycin antibiotic solution. The cells were grown as a monolayer at 37 °C in a 5% CO_2 atmosphere. For the transient transfections, Polyfect (301105; Qiagen, Germany) was used for the B16 cells and Viafect was used for the MM138 cells (E4981; Promega, USA).

2.3. Generation of the GFP-ShcD stable cell line

HEK 293 were first tested for their sensitivity to neomycin (G418), and 1 mg/ml was found to be sufficient to kill all of the cells. The cells were transfected with a GFP-ShcD-expressing construct carrying the neomycin-resistance gene. The transfected cells were then selected by applying 1 mg/ml neomycin (G418). The colonies that withstood the G418 treatment were harvested using cloning discs (Sigma) and then grown under the selective conditions for several passages. The surviving clones were tested for expression of the desired protein using western blotting. The stable cell lines were maintained in selective DMEM (containing 400 µg/ml G418) to ensure that the exogenous protein expression was maintained, although the cells were grown in neomycin-free DMEM before performing the experiments. The GFP-ShcD-expressing HEK 293 clone was called G5.

2.4. U0126 inhibitor and H_2O_2 treatment

B16 and MM138 cells were seeded in four 10-cm plates and then transfected when they reached 70% confluency. Twenty-four hours after transfection, two plates of cells were preincubated with 20 µM MEK kinase inhibitor (U0126) for 1 h, while the other two plates were treated with DMSO (vehicle control). One plate of U0126-treated cells and one plate of DMSO-treated cells were then treated with 5 mM H_2O_2 (ab120241; Abcam, UK) for 1 h. The other two plates were treated with a corresponding volume of sterile dH_2O, which was used for making the H_2O_2 dilution.

2.5. GFP-trap pulldowns

Cells were plated in ten 10-cm dishes and grown to 90% confluency; the cells were then lysed using 1 ml of ice-cold HiLO buffer (50 mM Tris pH 7.4, 0.825 M NaCl, 1% v/v NP-40, 1 mM PMSF, 1 mM Na_3VO_4, 50 mM NaF and a 1:100 dilution of protease inhibitor cocktail). The cells were incubated in HiLO buffer on ice for at least 1 min before they were scraped from the surface of the dish. After centrifugation of the cell lysate, the obtained clear cell lysate from ten 10-cm dishes was incubated with equilibrated beads [GFP-Trap-A (ChromoTek Inc., USA)] with gentle shaking at 4 °C for 2 h. The beads were washed, and SDS sample buffer was used to dissociate the precipitated protein complexes. The resolved proteins were then stained for 1 h with Instant Blue Coomassie (Expedeon; UK). The stained bands were excised from the gel and digested using trypsin. The samples were then analysed by performing liquid chromatography-tandem mass spectrometry (LC−MS/MS) with an Orbitrap instrument to assess the GFP-ShcD phosphorylation state (PNACL, University of Leicester, UK).

2.6. Co-immunoprecipitation

Transfected cells grown in a 10-cm plate were washed twice with pre-chilled PBS. The cells were then lysed for 10 min. with 500 µl of 1% Triton lysis buffer containing 50 mM sodium fluoride, 1 mM sodium vanadate, 1 mM PMSF and protease inhibitors. The cell lysate was collected by scraping, and the supernatant was collected after centrifugation of the lysate at 14,000 rpm for 10 min at 4 °C. The pellet was discarded, and 35 µg of protein from the whole-cell lysate (WCL) was loaded onto a 10% SDS-PAGE gel.

The rest of the supernatant from the cell lysate was incubated with protein G-sepharose 4B Fast Flow beads (Sigma; P3296) coupled to 3 µg of antibody. The mixture was left for 4 h in a cold room. The beads were washed 4 times with ice-cold 1% Triton lysis buffer. The bound proteins were then dissociated using 50 µl of 2X SDS-PAGE sample buffer with 100 mM DTT and boiled for 5–10 min at 100 °C.

2.7. In vitro non-radioactive ERK kinase assay

FLAG-tagged ShcD was expressed in MM138 melanoma cells, and the cell extracts were then added to a FLAG gel affinity column (A2220, Sigma Aldrich, UK) for purification. FLAG-ShcD was eluted using 0.1 M glycine HCl, pH 3.5, which was neutralized with 1 M Tris, pH 8.0. Five-hundred ng of purified FLAG-ShcD, MBP or FLAG peptide was used for the kinase assays, which were performed using an ADP-Glo Assay Kit (V9101, Promega, USA). A total of 0.2 µg of purified ERK2 (V1961, Promega; USA) and 50 µM ATP were added to the reactions. The reactions were terminated by adding ADP-Glo reagent, which depletes the remaining ATP. The addition of the kinase detection reagent converts any ADP to ATP and allows the freshly synthesized ATP to be detected via a luciferase/luciferin reaction. The luminescence level is proportional to the amount of ADP generated during the kinase reaction and was measured using a microplate reader (Thermo Scientific, USA).

2.8. Cell death assays

B16 and MM138 cells were seeded at a density of 50,000 cells/well in a 96-well plate. Following transfection with either FLAG-negative control vector or with FLAG-ShcD, the cells were treated with H_2O_2 and U0126 as described above. The caspase 3/7 assay was conducted following the manufacturer's instructions (G8090; Promega).

Cell death was also assessed by staining the cells with 7-Aminoactinomycin D (7-ADD) (ab176749; Abcam). Briefly, the cells were seeded on coverslips and then transfected with either empty vector or FLAG-ShcD. The treatment with U0126 and H_2O_2 were applied as previously indicated. The staining with 7-ADD was then performed. The cells were fixed with 2% Formaldehyde. The coverslips were mounted and sealed. A fluorescence microscope (Olympus microscope, BX51TF) was used to acquire the images. Five fields-of-view were obtained, and the stained cells were counted from blindly numbered slides. The percentage of dead cells out of the total number of cells (counted via DAPI-staining) was calculated, and the average values were plotted.

Cell viability was also assessed by employing Vybrant MTT cell proliferation assay kit (V13154; Invitrogen). The steps were followed as stated in the manufacturer's manual.

2.9. Statistical analysis

The data are expressed as the mean ± SE. The differences between the groups were examined for statistical significance using one-tailed Student's t-tests. $p < 0.05$ was considered statistically significant.

3. Results

3.1. Mass spectrometry analysis of ShcD phosphorylation following H_2O_2 treatment

Phosphorylation is crucial for intracellular signal propagation, protein regulation and the shuttling of proteins between intracellular compartments (Kholodenko, 2006; Acconcia et al., 2007). As described by Ahmed and Prigent, ShcD undergoes nuclear translocation in response to oxidative stress (Ahmed and Prigent, 2014). This observation prompted us to investigate the effect of oxidative stress on the ShcD phosphorylation status to determine whether phosphorylation explains the role of ShcD in the oxidative stress response. HEK 293 cell lines stably expressing GFP-ShcD were produced (Fig. 1Ai). GFP-trap was used to pull down the GFP-ShcD fusion protein in extracts of H_2O_2-treated or untreated GFP-ShcD-expressing HEK 293 cells (G5) (Fig. 1Aii). Untreated and untransfected HEK 293 cell extracts were also incubated with GFP-trap to confirm the specificity of GFP-ShcD pull-down (Fig. 1Aii).

The bands containing the immunoprecipitated GFP-ShcD (~100 kDa) from the H_2O_2-treated and untreated cell lysates (but not from the untransfected HEK 293 cell lysates) were excised, digested with trypsin, and analysed by LC−MS/MS. Spectrum analysis revealed ShcD phosphorylation at Thr159 in the TAL**T**^{159}PDS motif within the ShcD-CH2 domain (1-185 amino acids) in the H_2O_2-treated cells, while this modification was not detected in the untreated control cells (Fig. 1B). Furthermore, ShcD was found to be phosphorylated at Ser132 in the SGPS**S**^{132}PET motif in the ShcD-CH2 domain in both H_2O_2-treated and untreated cells (Fig. 1S, B). In this study, we decided to focus mainly on the Thr159 phosphorylation since it was only detected upon hydrogen peroxide treatment.

3.2. ShcD and MAPK interact under oxidative stress conditions

Like p66ShcA, ShcD has a CH2 domain that contains potential serine and threonine phosphorylation sites, which might be possible substrates for specific kinases. Since the Thr159 residue is in the CH2 domain, the CH2 sequence was screened for potential phosphorylation residues and their respective kinases using the GPS 2.1 phosphorylation prediction programme (Xue et al., 2011, 2008; Xue et al., 2005). The screening confirmed the prediction that Thr159 could be kinase-specific phosphorylation site and identified this residue as potential substrate for MAPKs (Table 1S). The next aim was to investigate whether ShcD forms a complex with MAPKs under oxidative stress conditions. FLAG-ShcD-transfected B16 melanoma cells were either treated for one hour with different H_2O_2 concentrations (0.25, 0.5, 1 or 5 mM) or left untreated. JNK, p38 and ERK all exhibited maximum phosphorylation after 5 mM H_2O_2 treatment (Fig. 2A). The FLAG-ShcD co-immunoprecipitated proteins were resolved on an SDS-PAGE gel. The most notable ShcD-MAPK interaction was observed for ERK. Interestingly, this interaction was observed with and without H_2O_2 treatment in the B16 melanoma cells. An antibody that detects phosphothreonine followed by a proline residue (phospho-Thr-P-Pro) detected a band that corresponded to FLAG-ShcD (Fig. 2A). To validate the ShcD/ERK interaction finding, the same experiment was repeated in transfected MM138 cells. In this case cells were also transfected with GFP-ERK. ERK/GFP-ERK were found to associate with FLAG-ShcD in both H_2O_2-treated and untreated MM138 cells, while the cells transfected with FLAG negative vector failed to pull down ERK/GFP-ERK (Fig. 2B).

3.3. ShcD is a potential ERK substrate in an in vitro kinase assay

To confirm that ShcD is directly phosphorylated by ERK, we performed ADP-Glo kinase assays by incubating active ERK2 with purified myelin basic protein (MBP, a known substrate of many MAPKs) and FLAG-ShcD; FLAG peptide was used as the negative control. The ADP-Glo assay measures the amount of ADP produced in the kinase reaction as an indirect measurement of substrate phosphorylation. Similar levels of luminescence were obtained using FLAG-ShcD or MBP as substrate. A weaker signal was observed with the FLAG peptide which does not represent phosphorylation of the peptide as it does not contain any serine or threonine residues. This could represent autophosphorylation of ERK in the kinase reaction. The luminescence obtained in the kinase assay with FLAG-ShcD as substrate was significantly different to that with FLAG peptide suggesting that ShcD is a direct substrate of ERK (Fig. 2C).

3.4. ERK inhibition enhanced its interaction with ShcD in response to H_2O_2 treatment

To gain better insight into the ShcD/ERK interaction, we analysed their interaction under oxidative stress conditions with or without U0126, an inhibitor of MEK, in two different cell lines; B16 and MM138. As observed previously, ShcD interacts with ERK under normal and stressful conditions. H_2O_2 treatment resulted in ERK phosphorylation; however, pre-treatment of the cells with U0126 blocked ERK

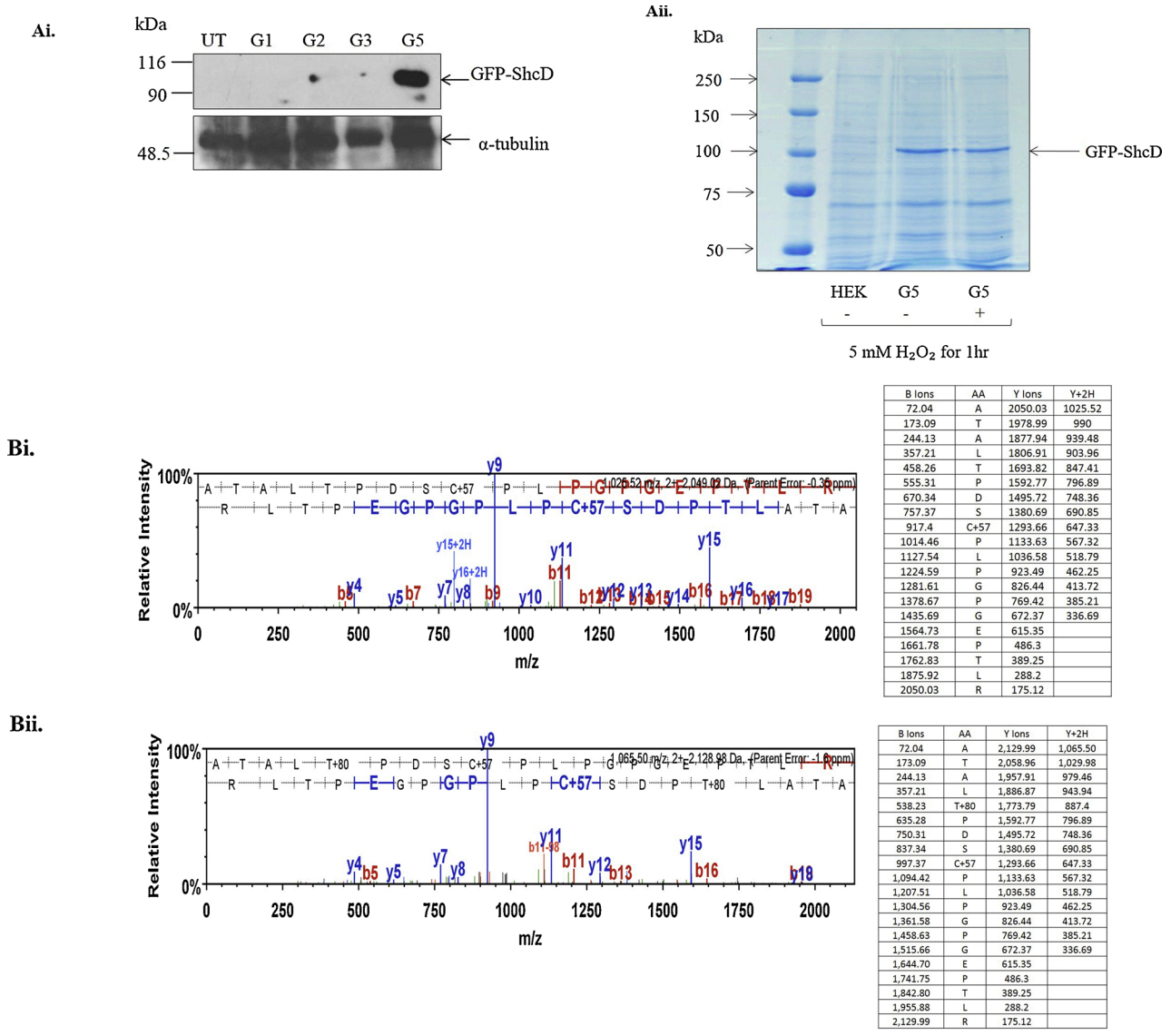

B Ions	AA	Y Ions	Y+2H
72.04	A	2050.03	1025.52
173.09	T	1978.99	990
244.13	A	1877.94	939.48
357.21	L	1806.91	903.96
458.26	T	1693.82	847.41
555.31	P	1592.77	796.89
670.34	D	1495.72	748.36
757.37	S	1380.69	690.85
917.4	C+57	1293.66	647.33
1014.46	P	1133.63	567.32
1127.54	L	1036.58	518.79
1224.59	P	923.49	462.25
1281.61	G	826.44	413.72
1378.67	P	769.42	385.21
1435.69	G	672.37	336.69
1564.73	E	615.35	
1661.78	P	486.3	
1762.83	T	389.25	
1875.92	L	288.2	
2050.03	R	175.12	

B Ions	AA	Y Ions	Y+2H
72.04	A	2,129.99	1,065.50
173.09	T	2,058.96	1,029.98
244.13	A	1,957.91	979.46
357.21	L	1,886.87	943.94
538.23	T+80	1,773.79	887.4
635.28	P	1,592.77	796.89
750.31	D	1,495.72	748.36
837.34	S	1,380.69	690.85
997.37	C+57	1,293.66	647.33
1,094.42	P	1,133.63	567.32
1,207.51	L	1,036.58	518.79
1,304.56	P	923.49	462.25
1,361.58	G	826.44	413.72
1,458.63	P	769.42	385.21
1,515.66	G	672.37	336.69
1,644.70	E	615.35	
1,741.75	P	486.3	
1,842.80	T	389.25	
1,955.88	L	288.2	
2,129.99	R	175.12	

Fig. 1. Phosphorylation of ShcD at Thr159 after H_2O_2 treatment. (A) Large-scale pull-down of GFP-ShcD from GFP-ShcD-expressing cells. (Ai) The HEK 293 cells were transfected with a construct encoding GFP-ShcD and a neomycin-resistance gene. The cells were treated with 1 mg/ml neomycin, and the neomycin-resistant clones (G5) were further grown and maintained. GFP-ShcD expression was confirmed by immunoblotting with anti-GFP antibody. (Aii) G5 cells were either treated with 5 mM H_2O_2 for 1 h or left untreated. Lysates obtained from treated G5, untreated G5 or untreated parental HEK 293 cells were incubated with GFP-trap. Immunoprecipitated GFP-ShcD was resolved on a 6% SDS-PAGE gel. The bands containing the GFP-ShcD immunoprecipitated with or without treatment were excised from the stained gel and sent for trypsinization and phosphopeptide analysis by LC−MS/MS. (B) The LC−MS/MS spectrum and fragmentation table indicate the detected b-ions and y-ions from the H_2O_2-treated (B, ii) and untreated (B, i) samples, n = 3. Scaffold 4 Proteomics Software was used to visualise the MS data.

phosphorylation, despite the subsequent H_2O_2 treatment (Fig. 3A & B). The immunoprecipitated proteins from the H_2O_2- and U0126-treated cells revealed the ShcD-ERK interaction in both the B16 and MM138 cell lines (Fig. 3A & B). To validate this result, MM138 cells were co-transfected with the FLAG-ShcD and GFP-ERK constructs, and the cells were treated as described above. Similarly, treatment of these cells with H_2O_2 and U0126 enhanced the interaction between FLAG-ShcD and GFP-ERK (Fig. 3B). Quantification of the ShcD and ERK interactions following the different treatments is shown in Fig. 3C. In the MM138 cells that were co-transfected with control vector (EV) and GFP-ERK, the anti-FLAG antibody was unable to pull down ERK or GFP-ERK, proving the specificity of the interaction between ShcD and ERK (Fig. 3B).

Moreover, phosphorylation of ShcD was examined using an anti-pThr-Pro antibody. A band corresponding to ShcD was detected by the antibody with H_2O_2 treatment, while the same band was not recognised when the cells were treated with U0126 and H_2O_2 (Fig. 3Ai). In summary, U0126 enhanced ShcD/ERK interaction and affected the phosphorylation status of ShcD under the 5 mM H_2O_2 treatment.

3.5. Introduction of the T159E mutation negatively impacted the ShcD/ERK interaction

To investigate the effect of ShcD Thr159 phosphorylation on the interaction between FLAG-ShcD and GFP-ERK, threonine 159 was mutated either to alanine (A) or to glutamic acid (E), and the interactions between the mutated proteins and GFP-ERK were then studied via co-immunoprecipitation with anti-FLAG antibody. Interestingly, it was found that introduction of the T159E mutation, which mimics phosphorylation, obliterated the ShcD-ERK interaction in H_2O_2-treated cells (Fig. 4). This finding was further studied by using GFP-trap to pull down GFP-ERK from lysates obtained from H_2O_2-treated cells co-expressing GFP-ERK and FLAG-ShcD (wild type (wt), T159E, or T159A) (Fig. 4). The result was consistent with the findings of the anti-FLAG

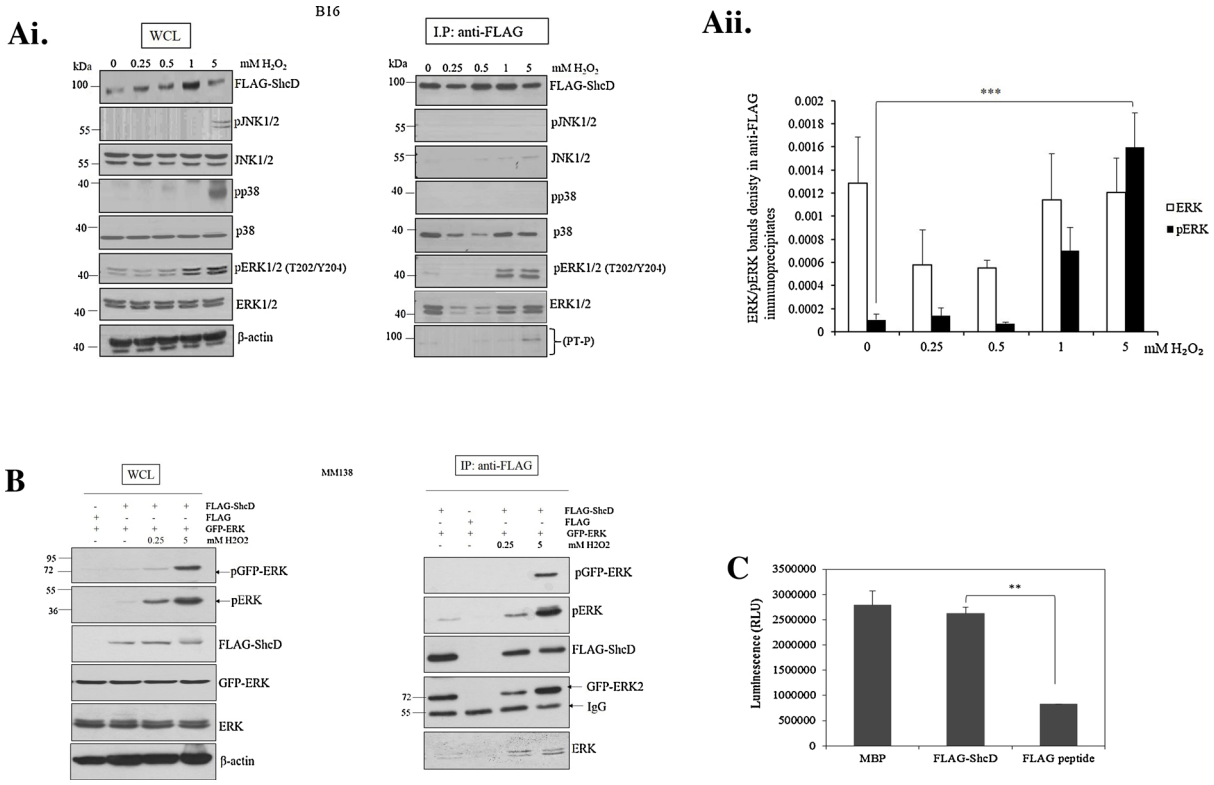

Fig. 2. ShcD is a potential ERK substrate. (A) B16 melanoma cells were transfected at 70% confluency with FLAG-ShcD. The cells were either left untreated or treated with different concentrations of H_2O_2 (0.25, 0.5, 1 or 5 mM) for 1 h. Next, the cells were lysed, and immunoprecipitation was performed using an anti-Flag antibody. The proteins immunoprecipitated from the whole cell lysate (WCL) with the anti-FLAG antibody were resolved on an 8% SDS-PAGE gel. The transferred proteins were probed with the antibodies indicated in A. PTP: phospho-threonine-proline. (B) MM138 melanoma cells were cotransfected with either FLAG negative control vector and GFP-ERK or with FLAG-ShcD and GFP-ERK. The cells were treated with 0.25- or 5-mM H_2O_2 or left untreated. The immunoprecipitated proteins with anti-FLAG antibody were resolved on an 8% SDS-PAGE gel. Immunoblotting was performed as indicated in B. (C) In vitro kinase assays indicate that ShcD is a potential ERK substrate. MBP was used as an ERK substrate, and FLAG peptide was used as a negative control for the kinase assay. MBP, purified FLAG-ShcD and FLAG peptide were incubated with 0.2 µg of ERK and 50 µM ATP. The generated luminescence is proportional to the ADP generated by the kinase (**p < 0.01).

coimmunoprecipitation experiments.

3.6. Overexpression of ShcD promotes modest ERK activation in the absence of H_2O_2 treatment

It was demonstrated in a previous report that ShcA has role in controlling ERK activity (Ranjbar and Holmes, 1996); therefore, experiments were designed to explore whether ShcD has any influence on the phosphorylation status of ShcD. MM138 cells were transfected with an empty vector (EV) or with FLAG-ShcD. The cells were then either treated with H_2O_2 or left untreated. Overexpression of ShcD induced a small, but significant increase in ERK phosphorylation in the absence of oxidative stress (Fig. 5).

3.7. ShcD and ERK activity affect survival following H_2O_2 treatment

To study the role of the ShcD and ERK interaction under acute oxidative stress conditions, B16 and MM138 cells were transfected either with FLAG-ShcD or with FLAG negative control vector (empty vector, EV). The cells were pre-treated with U0126 and then treated with H_2O_2. Cell death was measured in B16 cells using 7-AAD to measure late stage apoptosis and necrosis or a caspase 3/7 assay kit to measure apoptosis (Fig. 6). Using the 7-AAD assay, expression of ShcD promoted cell death on its own and this was enhanced by inhibition of ERK activation, suggesting a role for ERK in survival signalling. H_2O_2 further exacerbated cell death in ShcD transfected cells treated with U0126. H_2O_2 also induced cell death in cells transfected with empty vector, but with a significantly reduced effect, around 50% of the value in the ShcD expressing cells ($p < 0.05$). Surprisingly ERK inhibition by U0126 led to a decrease in cell death after H_2O_2 treatment only in the ShcD expressing cells. This suggests that ERK activation in response to H_2O_2 treatment may contribute to cell death in ShcD expressing cells (Fig. 6Ai, Aii). Using the caspase 3/7 assay to measure apoptosis, ShcD expression potentiated cell death in H_2O_2 -treated cells, although there was no significant effect of ERK inhibition (Fig. 6Bi, Bii).

Furthermore, the effect of ShcD mutants (T/A and T/E) on cell viability was tested (Fig. 6Ci, 6Cii). The expression of T159E ShcD mutant reduced the cell viability in H_2O_2-treated cells ($p < 0.01$ in B16 cells and $p < 0.05$ in MM138 cells). This finding is consistent with above experiment in which ShcD expression mediated cell death when the cells were treated with hydrogen peroxide, while the U0126 co-treatment resulted in less cell death.

To gain further insight into the implications of the ShcD-ERK interaction in cell survival, MM138 cells were ether transfected with EV or FLAG-ShcD, and the cells were treated as described previously. Immunoblotting against the phosphorylated form of the cyclin/cyclin-dependent kinase inhibitor p21, phosphorylated at T145 showed that it had increased phosphorylation in H_2O_2 -treated ShcD-expressing cells than in similarly treated cells transfected with the control vector (Fig. 7A). Treatment with U0126 prevented H_2O_2 induced p21 phosphorylation in cells transfected with ShcD or empty vector. To test if the rise in the p21 level is related to ShcD phosphorylation at Thr159, the p21 level was tested in T159E expressing cells. ShcDT159E mutant was observed to promote p21 expression and T145 phosphorylation when compared with the wild type and T159A mutant, while the T159A mutant overexpressing cells demonstrated low levels of p21 (Fig. 7B).

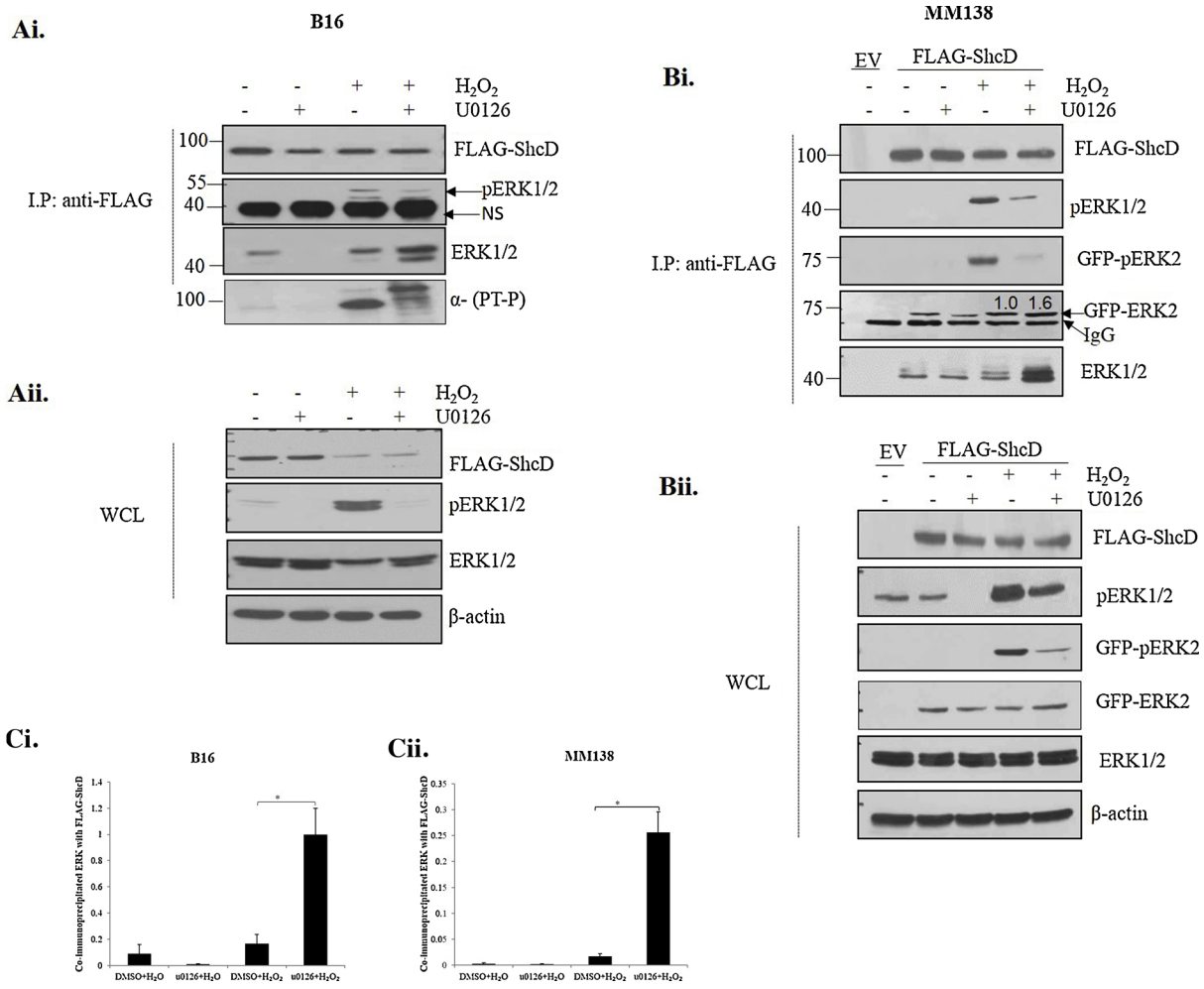

Fig. 3. ERK inhibition promoted the ShcD/ERK interaction. (A) B16 melanoma cells were transfected with FLAG-ShcD for 24 h. The cells were then treated with 20 μM U0126 for 1 h prior to treatment with 5 mM H_2O_2 for 2 h. The cell lysates were then incubated with immobilized FLAG-ShcD for 2 h. The whole cell lysates (WCL) in A and the co-immunoprecipitated proteins were resolved on an SDS-PAGE gel, and the transferred proteins were probed with the indicated antibodies, n = 4. (B) MM138 cells were cotransfected with either the empty vector containing a FLAG tag (EV) and GFP-ERK or with FLAG-ShcD and GFP-ERK. The melanoma cells were treated as described for B16 cells, and the blots were probed with the indicated antibodies, n = 2. (C) Quantification of co-immunoprecipitated ERK with FLAG-ShcD from transfected B16 and MM138 cells under different treatment conditions (n = 4 in case of B16 and n = 2 in case of MM138, *p < 0.05).

4. Discussion

ShcD is linked with ROS because it can translocate to the nucleus in response to 5 mM H_2O_2 treatment (Ahmed and Prigent, 2014). While this observation suggests a possible link between ShcD and the oxidative stress response, little is known about ShcD exact role in sever oxidative stress response. To delineate ShcD role in sever oxidative stress, it was decided initially to study its phosphorylation status by LC–MS/MS.

Oxidative stress is known to induce cell death particularly if it exceeds cell ability to neutralise excessive ROS generation. Despite the use of 5 mM H_2O_2 concentration might be considered high to study physiopathological cellular processes, a previous work by Bhat and Zhang unveiled that 5 mM H_2O_2 increased tyrosine phosphorylation more than all other used concentrations. In the same study, hydrogen peroxide higher than 1 mM activated ERK and p38 in CG4 glial cell line (Bhat and Zhang, 1999). A different published work has also reported that 5 mM H_2O_2 was sufficient to significantly suppress viral infection in Hela cells (Ranjbar and Holmes, 1996).

In this study, we have, for the first time, demonstrated that ShcD is an ERK substrate during the response to severe, acute oxidative stress. According to previous studies, p66ShcA is a substrate for JNK, p38 and ERK in response to various stressors, including H_2O_2 treatment, Taxol and UV light exposure (Migliaccio et al., 1999; Yang and Horwitz, 2002). The CH2 domain of ShcD contains MAP kinase recognition motifs (Thr159-Pro160 and Ser132-Pro133), indicating that ShcD is a potential substrate of MAPKs, which were also predicted by the GPS bioinformatics tool among others. Phosphorylation of ShcD-CH2 domain at Thr159 was detected by mass spectrometry mainly with hydrogen peroxide treatment unlike Ser132 phosphorylation that was detected in both untreated and treated samples; therefore, in this current work we decided to study the phosphorylation of ShcD at Thr159. This study confirmed that ShcD interacts with MAPKs, particularly with ERK, in both H_2O_2-treated and untreated cells. A significant interaction was observed with phosphorylated ERK following exposure to 5 mM H_2O_2; nevertheless, we cannot exclude the association of ShcD to other kinases under sever oxidative stress conditions. Intriguingly, blocking ERK activity promoted the interaction between ShcD and ERK, which is an expected consequence between inactive MAP kinases and their substrates (Cargnello and Roux, 2011). According to one interesting report, ShcA interacts with ERK via a direct interaction with ShcA-PTB and the N-terminal domain of ERK in the absence of growth factors, thus blocking signalling in the absence of growth factor stimuli (Suen et al., 2013). This observation might explain the interaction between ShcD and unphosphorylated ERK. In the same study, it was reported that ShcA phosphorylation leads to its dissociation from ERK, and in our

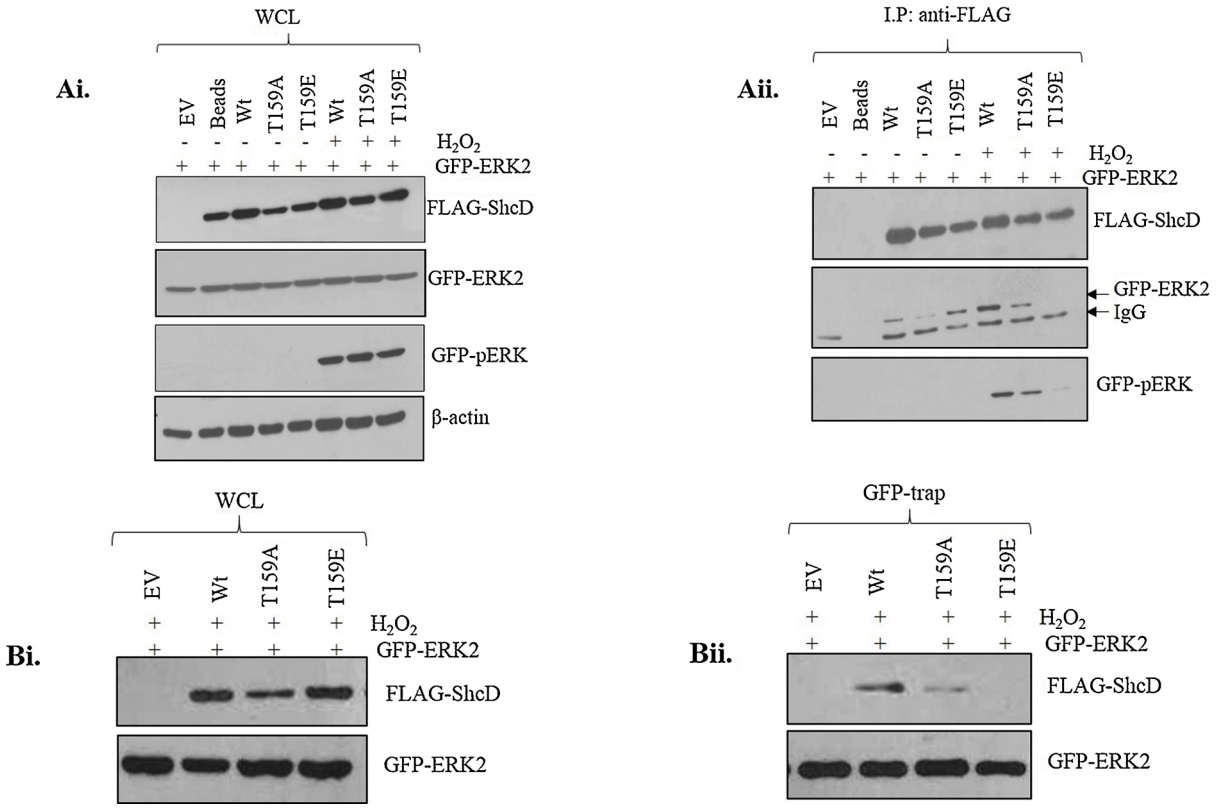

Fig. 4. ShcD phosphorylation negatively affects ShcD-ERK interaction. (A) MM138 cells were transfected with EV, WT FLAG-ShcD, T159A, or T159E. The cells were then treated with 5 mM H_2O_2 or left untreated. FLAG-ShcD and its mutants were immunoprecipitated with anti-FLAG antibody. The coimmunoprecipitated GFP-ERK was detected with an anti-GFP antibody. Whole cell lysates (WCL) were immunoblotted with the indicated antibodies to confirm the transfections and the efficiency of the H_2O_2 treatment. (B) MM138 cells were cotransfected with EV and GFP-ERK, or with wild type FLAG-ShcD (wt), T159A, or T159E and GFP-ERK. GFP-ERK was immunoprecipitated via GFP-trap from the transfected, H_2O_2-treated MM138 cells. The co-immunoprecipitated ShcD and its mutants were detected with an anti-FLAG antibody.

study, the phosphorylation of Thr159 resulted in dissociation of the ShcD/ERK complex. ShcD was also shown to bind the epidermal growth factor receptor in the absence of ligand binding via its ShcD-PTB domain. This interaction mediated EGFR phosphorylation at the Y1068 motif independent of ligand stimulation (Wills et al., 2014). These reported findings provide evidence of a direct relationship between Shc proteins and their kinases in the absence of kinase stimulation.

Our data showed that there is no evidenced increase in ShcD/ERK interaction when the cells treated with 0.25 and 0.5 mM when compared to the higher concentrations of H_2O_2; this could be explained by the fact that ERK might be involved in a different pathway that is responsible for restoring the cellular wellbeing. Severe oxidative stress condition such as 1 mM was able to initiate cellular death via ERK activation (Lee et al., 2003). ShcD possibly facilitates ERK-mediated cellular death in melanoma cells under oxidative stress condition. The role of p66ShcA in inducing pro-apoptotic signal under oxidative stress has already been proven, which indeed supports ShcD-induced cellular death when the cells are exposed to high concentrations of hydrogen peroxide or possibly after chemotherapy treatment (Bhat et al., 2015). Further studies are indeed needed to understand the mechanistic role of ShcD and ERK interaction in different hydrogen peroxide concentrations.

Substrate-kinase relationships have been studied over many decades. It has been shown that a kinase has a higher affinity to the unphosphorylated substrate (Sommese and Sivaramakrishnan, 2016), which explains the diminution of ERK/T159EShcD interaction, the latter mimicking the phosphorylated version of the substrate. The fact that our data demonstrated that ERK-ShcD interaction has increased upon U0126, it shows that the affinity of ShcD to the unphosphorylated ERK is not affected by U0126. The unphosphorylated ERK interacted similarly to ShcD under both 5 mM H_2O_2 treated and untreated conditions. Moreover, under the severe oxidative stress U0126 inhibits the ability of ERK to phosphorylate ShcD; however, ERK's ability to bind ShcD remains unaffected.

ERK is known for its role in cell survival in the presence of growth factors and under certain stressful conditions (Aikawa et al., 1997; Lu and Xu, 2006). However, according to some reports, ERK induces apoptosis under various stress conditions, including oxidative stress (Wang et al., 2000; Tan and Chiu, 2013). Our findings revealed that the ShcD/ERK interaction promotes cell death upon oxidative stress, which might indicate that ShcD is a key factor in the ERK-mediated oxidative stress response. The p66ShcA Ser36 mutation to a non-phosphorylatable amino acid results in resistance to apoptosis under increased ROS conditions (Masgras et al., 2012); consistent to this our data showed that mutant ShcD (T/E) favoured cell death upon hydrogen peroxide treatment. Notably, the Thr159 residue in the ShcD-CH2 domain is not conserved among the other Shc family members (Fig. 2S), hinting at a unique function for ShcD during oxidative stress.

ROS can play a role as a second messenger in cancer development and at the same time elevated levels of ROS is a known mechanism of how chemotherapeutic agents kill cancer cells. In this study, 5 mM of hydrogen peroxide was used, and this possibly describes the moment of no return and death is an inevitable fate. In mild to moderate oxidative stress p21 was reported to neutralise intracellular ROS by Nrf2 antioxidant, whereas in case of sever oxidative stress p21 fails to initiate Nrf2 antioxidant effect; thereby cells die (Villeneuve et al., 2009). In addition, p21 was reported to mediate cellular death following treatment with various chemotherapeutic agents as well as oxidative stress (Davies et al., 2015; Masgras et al., 2012). Phosphorylation of Thr145 at the c-terminus of p21 is linked to p21 stability and its cytoplasmic

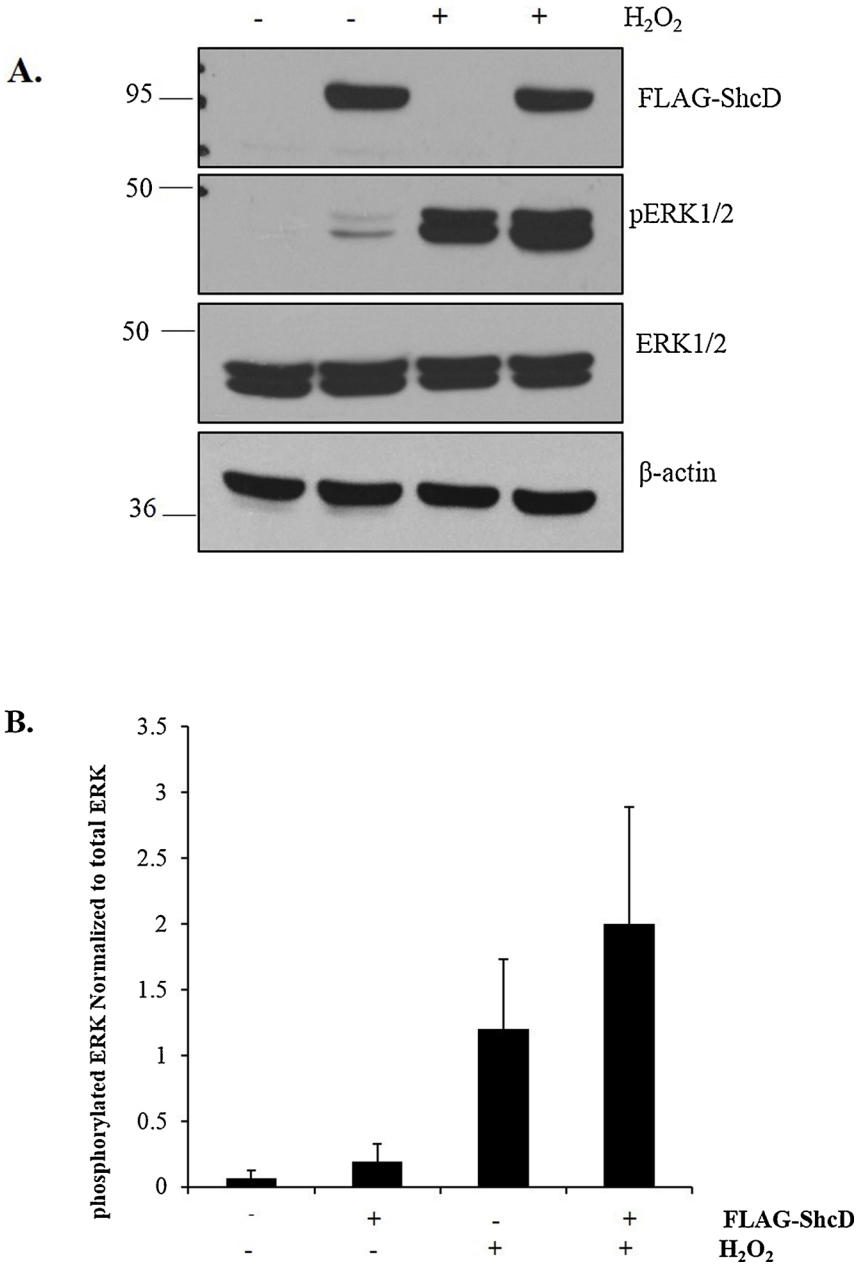

Fig. 5. ShcD promotes ERK phosphorylation under normal and oxidative stress conditions. (A) MM138 cells were either transfected with EV or FLAG-ShcD. The cells were either left untreated or treated with H_2O_2. The obtained cell lysates were immunoblotted with the indicated antibodies. A pool of two experiments was plotted, as shown in (B).

localisation (Zhang et al., 2007). Additionally, p21 Thr145 phosphorylation was reported to have role in chemotherapeutic resistance and cell survival (Koster et al., 2010). In contrast to this, cytoplasmic p21 and its c-terminus were linked to apoptosis promotion in oxidative stress conditions (Dong et al., 2005). In the work presented here, high levels of hydrogen peroxide treatment caused elevation of p21 levels in ShcD-overexpressing cells and this ultimately resulted in increase of cell death, which contradict the anti-apoptotic role of p21 while it matches its role in apoptosis in extreme oxidative stress conditions. In unpublished work by Ahmed and Prigent stable expression of FLAG-ShcD by HEK 293 cells resulted in higher levels of p21 when compared with the counterparts. Further experiments are indeed needed to explore the ShcD/p21 axis and their role in the cellular fate.

5. Conclusion

Shc proteins are recognized for their role in transducing extracellular signals into the internal environment of the cell, and p66ShcA has an interesting function in the oxidative stress response. In this study, the most recently identified Shc adaptor, ShcD, appears to be involved in the oxidative stress response in addition to p66ShcA. ShcD was shown to interact with phosphorylated ERK upon oxidative stress, although ShcD and ERK also interacted under non-oxidative stress conditions, an observation that needs additional prudent investigation. The interaction between ShcD and ERK was shown to mediate death signalling under severe oxidative stress conditions, a function that contradicts ERK's role in promoting cell survival.

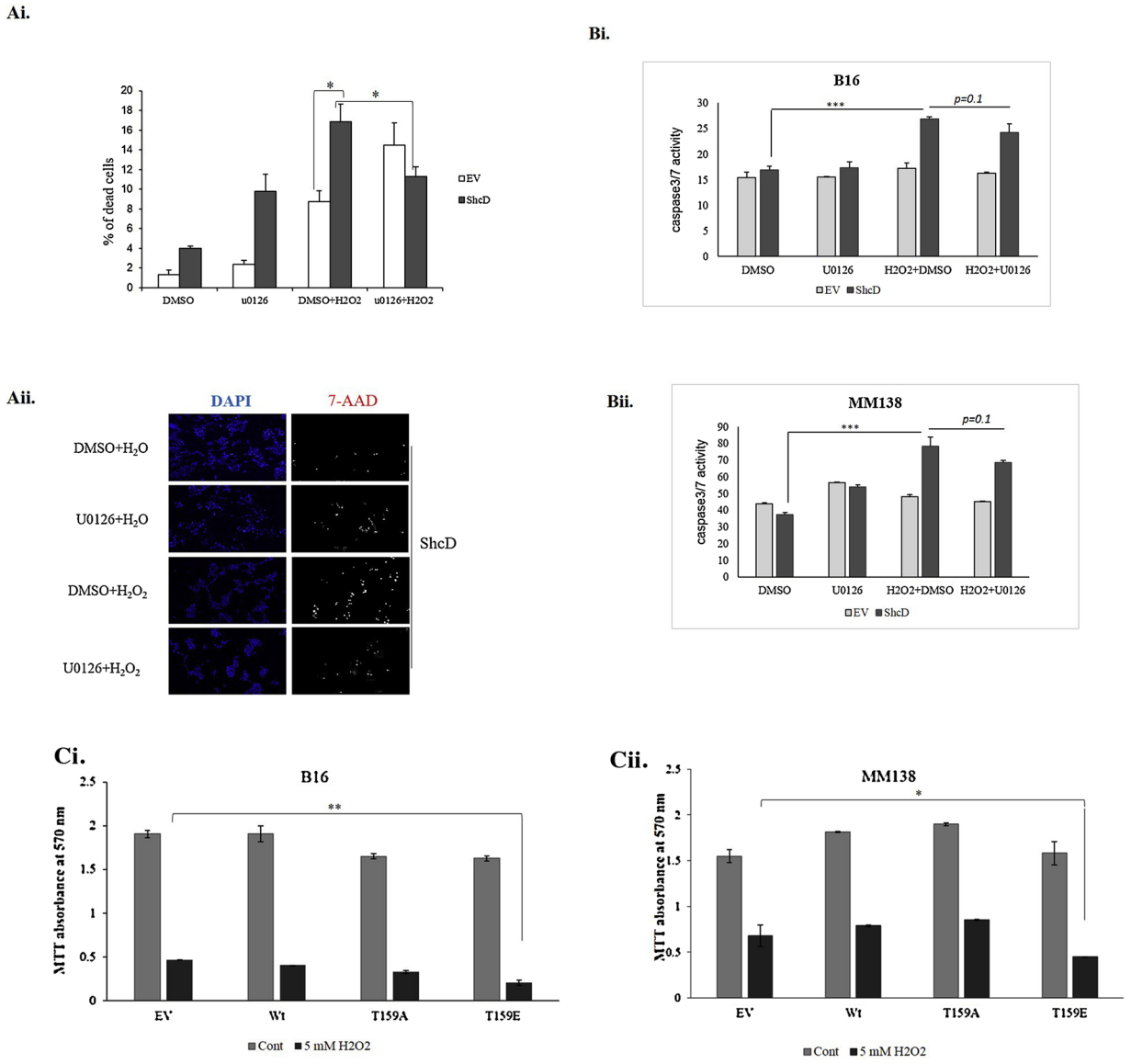

Fig. 6. The effect of the ShcD and ERK interaction on cell survival. (A) B16 cells were grown on coverslips and then transfected with EV or FLAG-ShcD. The cells were either left untreated, treated with U0126 or 5 mM H_2O_2, or with 5 mM H_2O_2 and U0126. The cells were then stained with 7-aminoactionomycin D. The images were acquired with a fluorescence microscope. The percentages of the dead cells are shown in Ai from a pool of 2 experiments and 5 fields-of-view from each experiment. (Aii) Representative of images obtained from ShcD-transfected B16 cells. (B) B16 and MM138 cells were transfected and treated similarly to those in A. Cell apoptosis was assessed by measuring caspase3/7 activity. (Bi) n = 2. (Bii) n = 2. (C) 5×10^4 of transfected B16 or MM138 cells were seeded in 96 wells plate for 24 h. One set of cells was left untreated, indicated as Cont (dH2O was added instead of H_2O_2), and the second set was treated with 5 mM H_2O_2 for 2 h. The cells were then washed with PBS and the MTT substrate was added for 4 h. The formazan precipitate was incubated with SDS for 16 h and the reading were taken at 570 nm. N = 2 for each of the cell lines ($p < 0.05$ *, $p < 0.01$**).

Conflicts of interest

The authors declare no conflicts of interest.

Funding

This project was funded by a Seed Grant from the Al Jalila Foundation, Dubai-UAE (AJF201636). A University of Leicester PhD scholarship funded the mass spectrometry experiment. Preliminary data for this project were obtained from a student grant from Boehringer Ingelheim.

Author contributions

Samrein Ahmed designed most of the experiments, performed the mass spectrometry, generated the mutations, and was involved in performing the remainder of the experiments. She also wrote the manuscript and analysed the data.

Sara Amer and Mira Emad participated in performing the preliminary experiments.

Mohamed Rahmani proofread the paper and provided some valuable comments

Sally Prigent provided the FLAG-ShcD construct. The HEK 293 stable cell lines were established and the mass spectrometry was performed under her supervision at the University of Leicester, UK. She also proofread the manuscript.

Acknowledgments

Our sincere thanks go to Dr. Andrew Botrill and Ms. Ashra

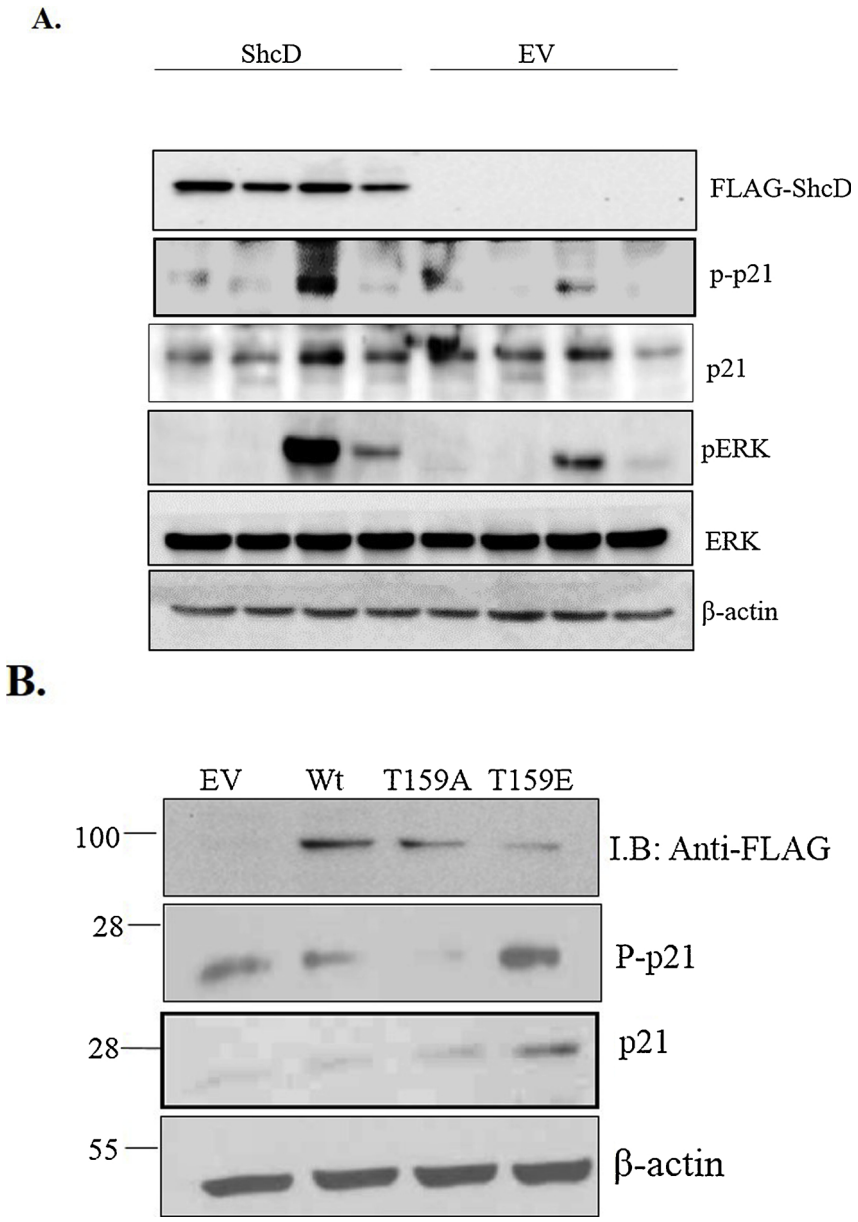

Fig. 7. ShcD expression induces p21 phosphorylation in response to H_2O_2 treatment. MM13 cells were transfected with either ShcD or EV. The cells were then left untreated or treated with U0126 or H_2O_2 or with H_2O_2 and U0126 together. The cell lysates were immunoblotted with the indicated antibodies. n = 2. (B) MM138 were transfected with empty vector (EV), ShcD (Wt), ShcD mutant T159A or ShcD mutant T159E. The cells were then lysed and the extracted proteins were immunoblotted with the indicated antibodies.

Shairbanu (PNACL service, University of Leicester, UK), who provided technical assistance with the mass spectrometry experiment. We would like to thank Asha Caroline Thomas, Keerthi Rajan and Nour Shawa for their technical assistance in some of the experiments.

Appendix A. Supplementary data

Supplementary material related to this article can be found, in the online version, at doi:https://doi.org/10.1016/j.biocel.2019.05.009.

References

Acconcia, F., Barnes, C.J., Singh, R.R., Talukder, A.H., Kumar, R., 2007. Phosphorylation-dependent regulation of nuclear localization and functions of integrin-linked kinase. Proc. Natl. Acad. Sci. U. S. A. 104 (16), 6782–6787.

Ahmed, S.B., Prigent, S.A., 2014. A nuclear export signal and oxidative stress regulate ShcD subcellular localisation: a potential role for ShcD in the nucleus. Cell Signal. 26 (1), 32–40.

Aikawa, R., Komuro, I., Yamazaki, T., Zou, Y., Kudoh, S., Tanaka, M., et al., 1997. Oxidative stress activates extracellular signal-regulated kinases through Src and Ras in cultured cardiac myocytes of neonatal rats. J. Clin. Invest. 100 (7), 1813–1821.

Belikov, A.V., Schraven, B., Simeoni, L., 2015. T cells and reactive oxygen species. J. Biomed. Sci. 22, 85.

Bhat, S.S., Anand, D., Khanday, F.A., 2015. p66Shc as a switch in bringing about contrasting responses in cell growth: implications on cell proliferation and apoptosis. Mol. Cancer 14, 76.

Bhat, N.R., Zhang, P., 1999. Hydrogen peroxide activation of multiple mitogen-activated protein kinases in an oligodendrocyte cell line: role of extracellular signal-regulated kinase in hydrogen peroxide-induced cell death. J. Neurochem. 72 (1), 112–119.

Cargnello, M., Roux, P.P., 2011. Activation and function of the MAPKs and their substrates, the MAPK-activated protein kinases. Microbiol. Mol. Biol. Rev. 75 (1), 50–83.

Davies, C., Hogarth, L.A., Mackenzie, K.L., Hall, A.G., Lock, R.B., 2015. p21(WAF1) modulates drug-induced apoptosis and cell cycle arrest in B-cell precursor acute lymphoblastic leukemia. Cell Cycle 14 (22), 3602–3612.

Dong, C., Li, Q., Lyu, S.C., Krensky, A.M., Clayberger, C., 2005. A novel apoptosis pathway activated by the carboxyl terminus of p21. Blood 105 (3), 1187–1194.

Emerit, J., Edeas, M., Bricaire, F., 2004. Neurodegenerative diseases and oxidative stress. Biomed. Pharmacother. 58 (1), 39–46.

Esme, H., Cemek, M., Sezer, M., Saglam, H., Demir, A., Melek, H., et al., 2008. High levels of oxidative stress in patients with advanced lung cancer. Respirology 13 (1),

112–116.
Fagiani, E., Giardina, G., Luzi, L., Cesaroni, M., Quarto, M., Capra, M., et al., 2007. RaLP, a new member of the Src homology and collagen family, regulates cell migration and tumor growth of metastatic melanomas. Cancer Res. 67 (7), 3064–3073.
Giorgio, M., Migliaccio, E., Orsini, F., Paolucci, D., Moroni, M., Contursi, C., et al., 2005. Electron transfer between cytochrome c and p66Shc generates reactive oxygen species that trigger mitochondrial apoptosis. Cell 122 (2), 221–233.
Hori, M., Nishida, K., 2009. Oxidative stress and left ventricular remodelling after myocardial infarction. Cardiovasc. Res. 81 (3), 457–464.
Hu, Y., Wang, X., Zeng, L., Cai, D.Y., Sabapathy, K., Goff, S.P., et al., 2005. ERK phosphorylates p66shcA on Ser36 and subsequently regulates p27kip1 expression via the Akt-FOXO3a pathway: implication of p27kip1 in cell response to oxidative stress. Mol. Biol Cell. 16 (8), 3705–3718.
Khalid, S., Drasche, A., Thurner, M., Hermann, M., Ashraf, M.I., Fresser, F., et al., 2016. cJun N-terminal kinase (JNK) phosphorylation of serine 36 is critical for p66Shc activation. Sci. Rep. 6, 20930.
Kholodenko, B.N., 2006. Cell-signalling dynamics in time and space. Nat. Rev. Mol. Cell. Biol. 7 (3), 165–176.
Koster, R., di Pietro, A., Timmer-Bosscha, H., Gibcus, J.H., van den Berg, A., Suurmeijer, A.J., et al., 2010. Cytoplasmic p21 expression levels determine cisplatin resistance in human testicular cancer. J. Clin. Invest. 120 (10), 3594–3605.
Kregel, K.C., Zhang, H.J., 2007. An integrated view of oxidative stress in aging: basic mechanisms, functional effects, and pathological considerations. Am. J. Physiol. Regul. Integr. Comp. Physiol. 292 (1), R18–36.
Lee, Y.J., Cho, H.N., Soh, J.W., Jhon, G.J., Cho, C.K., Chung, H.Y., et al., 2003. Oxidative stress-induced apoptosis is mediated by ERK1/2 phosphorylation. Exp. Cell Res. 291 (1), 251–266.
Lu, Z., Xu, S., 2006. ERK1/2 MAP kinases in cell survival and apoptosis. IUBMB Life 58 (11), 621–631.
Martindale, J.L., Holbrook, N.J., 2002. Cellular response to oxidative stress: signaling for suicide and survival. J. Cell Physiol. 192 (1), 1–15.
Masgras, I., Carrera, S., de Verdier, P.J., Brennan, P., Majid, A., Makhtar, W., et al., 2012. Reactive oxygen species and mitochondrial sensitivity to oxidative stress determine induction of cancer cell death by p21. J. Biol. Chem. 287 (13), 9845–9854.
Matos, T.J., Duarte, C.B., Goncalo, M., Lopes, M.C., 2005. Role of oxidative stress in ERK and p38 MAPK activation induced by the chemical sensitizer DNFB in a fetal skin dendritic cell line. Immunol. Cell. Biol. 83 (6), 607–614.
Migliaccio, E., Giorgio, M., Mele, S., Pelicci, G., Reboldi, P., Pandolfi, P.P., et al., 1999. The p66shc adaptor protein controls oxidative stress response and life span in mammals. Nature 402 (6759), 309–313.
Nemoto, S., Finkel, T., 2002. Redox regulation of forkhead proteins through a p66shc-dependent signaling pathway. Science 295 (5564), 2450–2452.
Ranjbar, S., Holmes, H., 1996. Influence of hydrogen peroxide on the in vitro infectivity of human immunodeficiency virus. Free Radic. Biol. Med. 20 (4), 573–577.
Ravichandran, K.S., 2001. Signaling via Shc family adapter proteins. Oncogene 20 (44), 6322–6330.
Ruffels, J., Griffin, M., Dickenson, J.M., 2004. Activation of ERK1/2, JNK and PKB by hydrogen peroxide in human SH-SY5Y neuroblastoma cells: role of ERK1/2 in H2O2-induced cell death. Eur. J. Pharmacol. 483 (2-3), 163–173.
Sommese, R.F., Sivaramakrishnan, S., 2016. Substrate affinity differentially influences protein kinase C regulation and inhibitor potency. J. Biol. Chem. 291 (42), 21963–21970.
Suen, K.M., Lin, C.C., George, R., Melo, F.A., Biggs, E.R., Ahmed, Z., et al., 2013. Interaction with Shc prevents aberrant Erk activation in the absence of extracellular stimuli. Nat. Struct. Mol. Biol. 20 (5), 620–627.
Tan, B.J., Chiu, G.N., 2013. Role of oxidative stress, endoplasmic reticulum stress and ERK activation in triptolide-induced apoptosis. Int. J. Oncol. 42 (5), 1605–1612.
Trachootham, D., Lu, W., Ogasawara, M.A., Nilsa, R.D., Huang, P., 2008. Redox regulation of cell survival. Antioxid. Redox Signal. 10 (8), 1343–1374.
Villeneuve, N.F., Sun, Z., Chen, W., Zhang, D.D., 2009. Nrf2 and p21 regulate the fine balance between life and death by controlling ROS levels. Cell. Cycle 8 (20), 3255–3256.
Wang, X., Martindale, J.L., Holbrook, N.J., 2000. Requirement for ERK activation in cisplatin-induced apoptosis. J. Biol. Chem. 275 (50), 39435–39443.
Wang, M.C., Bohmann, D., Jasper, H., 2003. JNK signaling confers tolerance to oxidative stress and extends lifespan in Drosophila. Dev. Cell 5 (5), 811–816.
Wang, X., Liu, J.Z., Hu, J.X., Wu, H., Li, Y.L., Chen, H.L., et al., 2011. ROS-activated p38 MAPK/ERK-Akt cascade plays a central role in palmitic acid-stimulated hepatocyte proliferation. Free Radic. Biol. Med. 51 (2), 539–551.
Wang, H., Gao, Z., Liu, X., Agarwal, P., Zhao, S., Conroy, D.W., et al., 2018. Targeted production of reactive oxygen species in mitochondria to overcome cancer drug resistance. Nat. Commun. 9 (1), 562.
Wills, M.K., Tong, J., Tremblay, S.L., Moran, M.F., Jones, N., 2014. The ShcD signaling adaptor facilitates ligand-independent phosphorylation of the EGF receptor. Mol. Biol Cell 25 (6), 739–752.
Xue, Y., Zhou, F., Zhu, M., Ahmed, K., Chen, G., Yao, X., 2005. GPS: a comprehensive www server for phosphorylation sites prediction. Nucleic Acids Res. 33 (Web Server issue), W184–7.
Xue, Y., Ren, J., Gao, X., Jin, C., Wen, L., Yao, X., 2008. GPS 2.0, a tool to predict kinase-specific phosphorylation sites in hierarchy. Mol. Cell. Proteom. 7 (9), 1598–1608.
Xue, Y., Liu, Z., Cao, J., Ma, Q., Gao, X., Wang, Q., et al., 2011. GPS 2.1: enhanced prediction of kinase-specific phosphorylation sites with an algorithm of motif length selection. Protein Eng. Des. Sel. 24 (3), 255–260.
Yang, C.P., Horwitz, S.B., 2002. Distinct mechanisms of taxol-induced serine phosphorylation of the 66-kDa Shc isoform in A549 and RAW 264.7 cells. Biochim. Biophys. Acta 1590 (1-3), 76–83.
Zhang, Y., Wang, Z., Magnuson, N.S., 2007. Pim-1 kinase-dependent phosphorylation of p21Cip1/WAF1 regulates its stability and cellular localization in H1299 cells. Mol. Cancer Res. 5 (9), 909–922.
Zhou, Y., Wang, Q., Evers, B.M., Chung, D.H., 2005. Signal transduction pathways involved in oxidative stress-induced intestinal epithelial cell apoptosis. Pediatr. Res. 58 (6), 1192–1197.
Zhuang, S., Yan, Y., Daubert, R.A., Han, J., Schnellmann, R.G., 2007. ERK promotes hydrogen peroxide-induced apoptosis through caspase-3 activation and inhibition of Akt in renal epithelial cells. Am. J. Physiol. Ren. Physiol. 292 (1), F440–7.